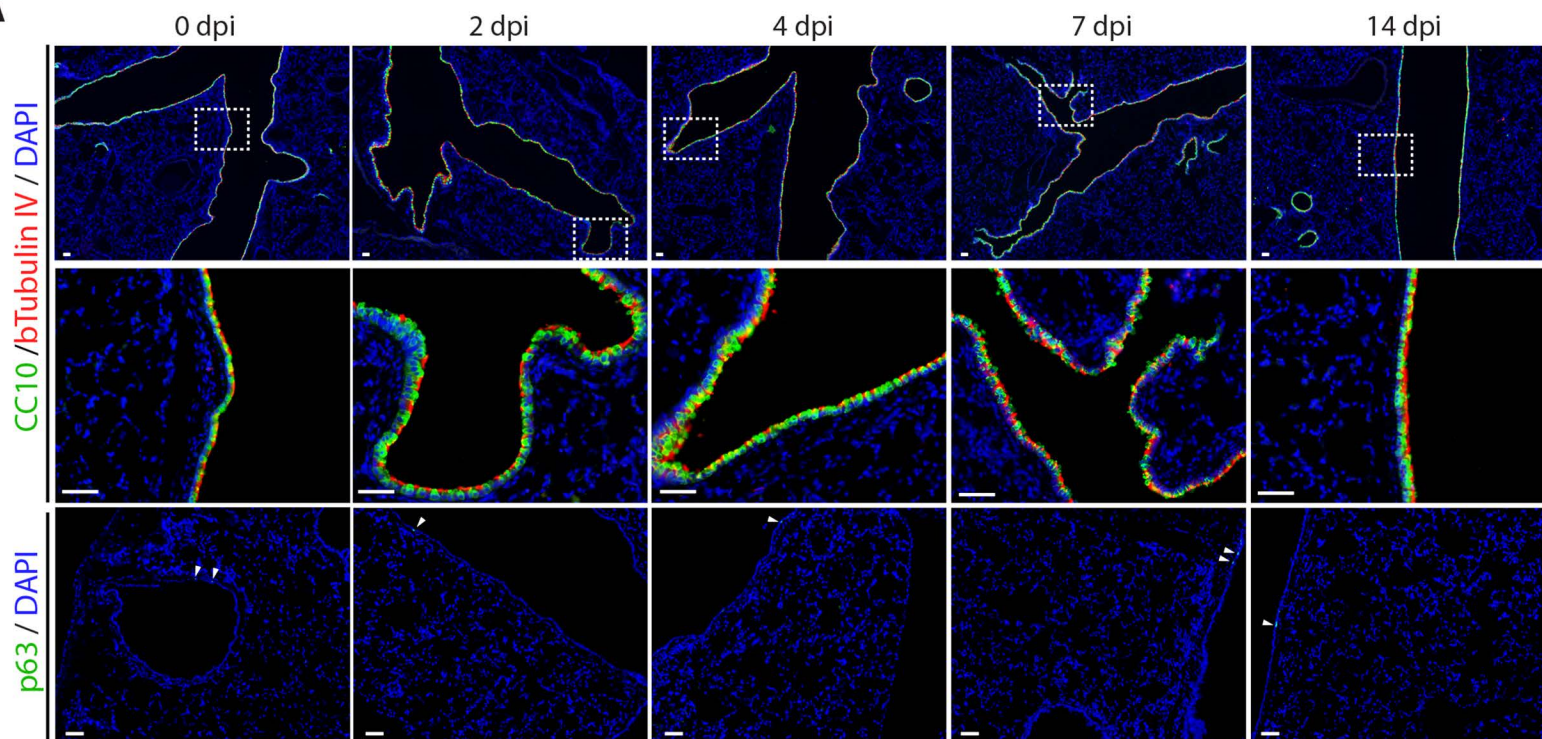
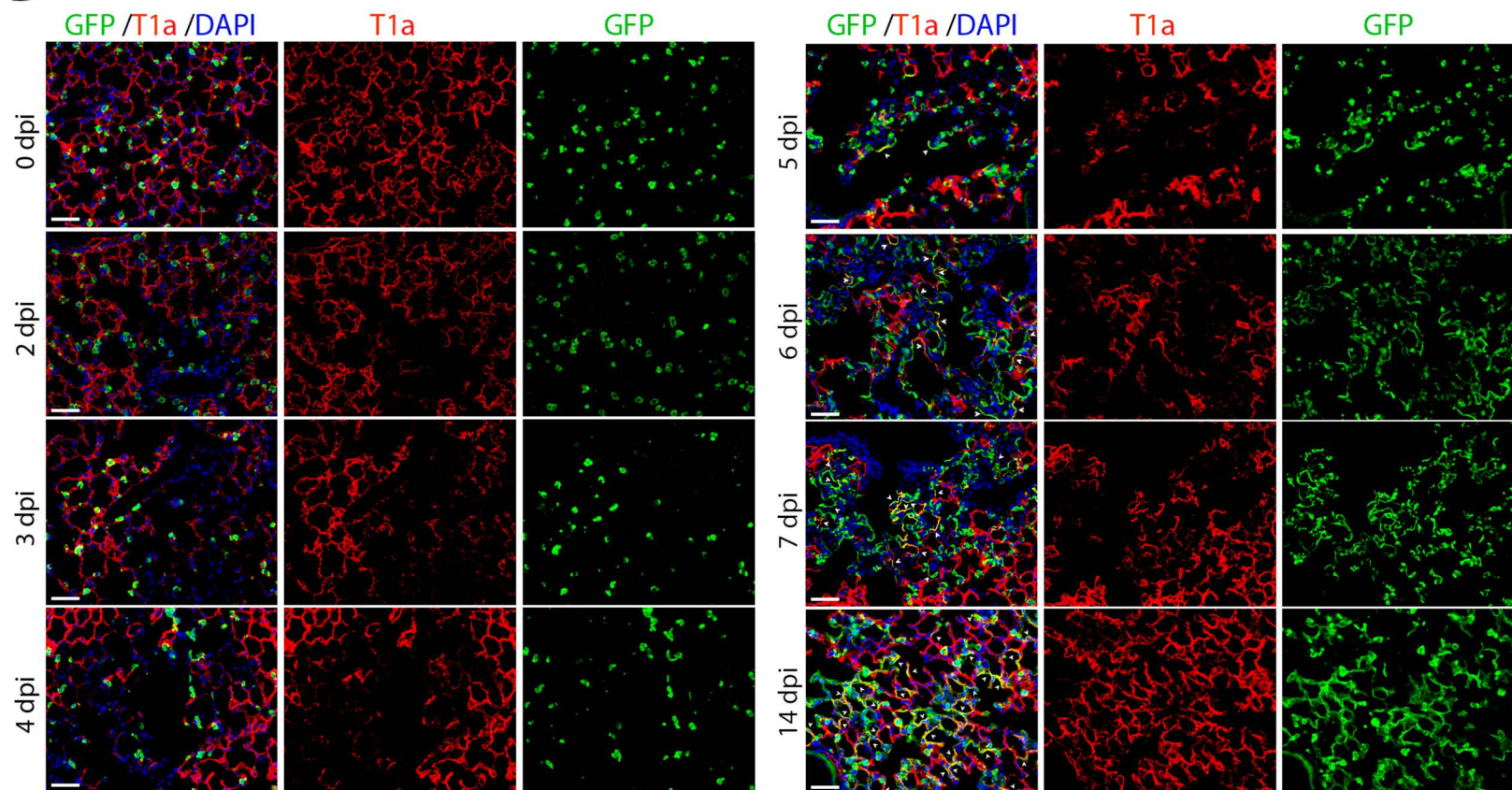


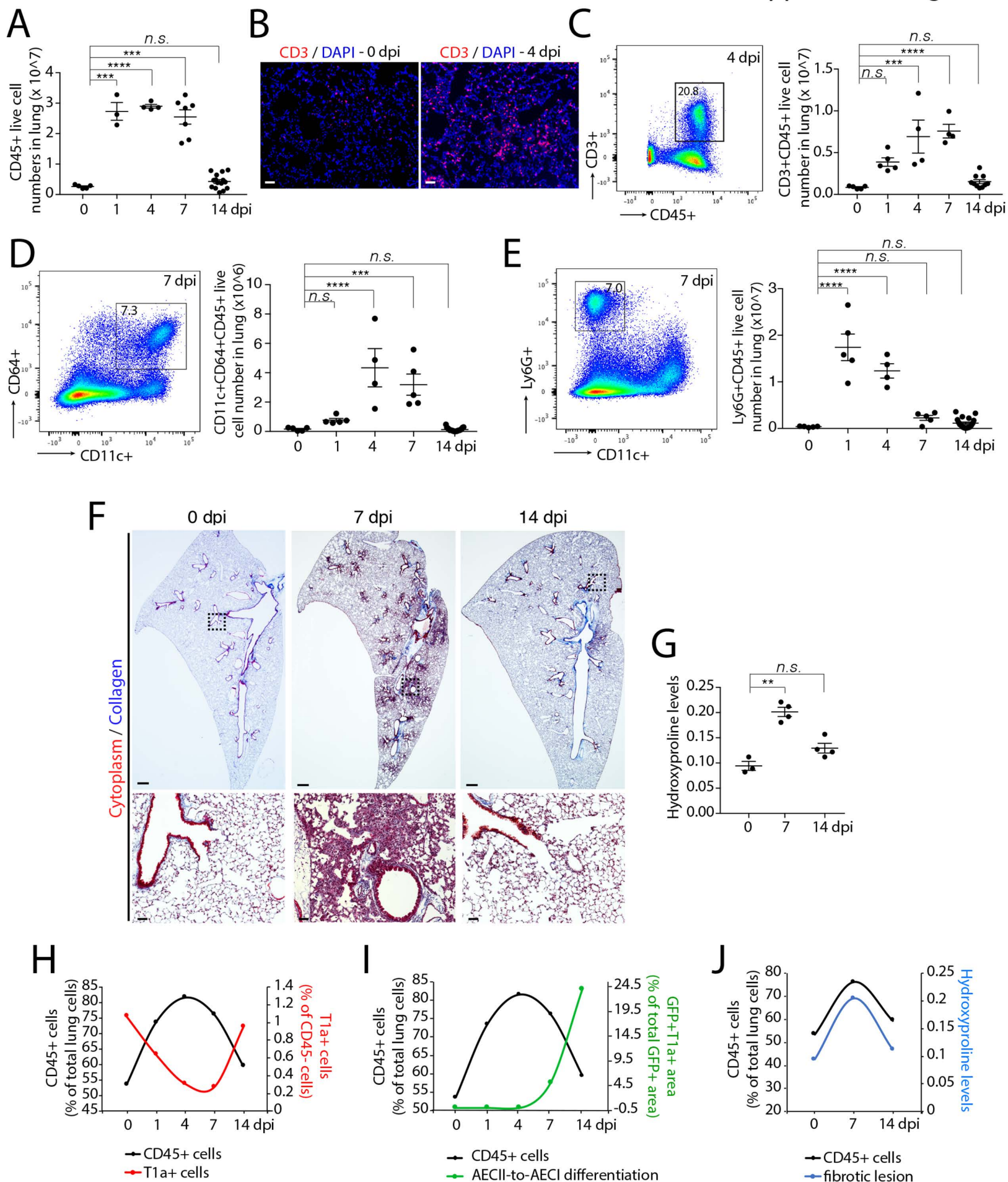
A



B



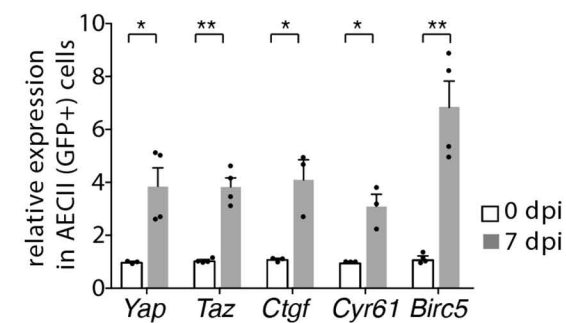
Supplemental Figure 1. Characterization of SpT4-infected mouse lungs. (A) Immunostaining on lung sections with antibodies to CC10 (green), bTubulin IV (red), and p63 (green). Cell nuclei were stained with DAPI (blue). Arrows in p63/DAPI images indicated p63+ cells. (B) Lineage tracing of SPC+ AECIIs following SpT4 infection. Adult SPC-CreERT2, Rosa26-mTmG mice were treated with 3 doses of tamoxifen (i.p.) to label SPC+ AECIIs. Fourteen days after the last tamoxifen treatment, mice were infected with SpT4. Lung tissues sections were obtained at progressive dpi and immune-stained with antibodies to GFP (green) and T1a (red) and DNA counterstain (DAPI, blue). Scale bars: 50 μ m.



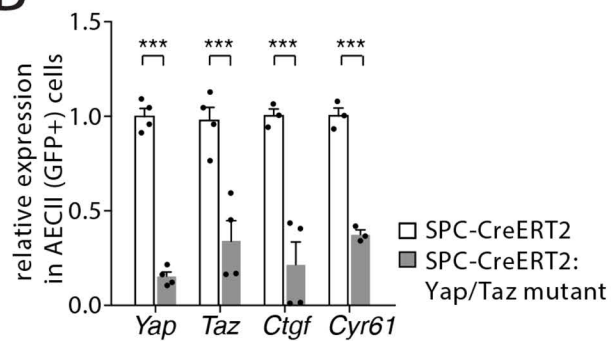
Supplemental Figure 2. Inflammatory resolution in mouse lungs after SpT4 infection. (A)

Quantification of the number of inflammatory cells (CD45+) in the lung using flow cytometry (n=3-15 per group). (B) Immunostaining on lung sections with antibody against CD3 (red), with nuclei labeled by DAPI (blue). (C) Quantification of the number of T cells (CD3+CD45+) in the lung using flow cytometry. (D) Flow cytometry of dissociated lung cells at 7 dpi were performed by gating on CD11c+CD64+CD45+ cells (left panel). Quantification of the number of CD11c+CD64+CD45+ cells in the lung (right panel). (E) Flow cytometry of dissociated lung cells at 7 dpi were performed by gating on Ly6G+CD45+ cells (left panel). Quantification of the number of Ly6G+CD45+ cells in the lung (right panel). (F) Lung sections were stained with Alcian blue and nuclear fast red. (G) Quantification of collagen level on lung tissue lysates using hydroxyproline assay. (H-J) Graphics depicts overall trend of lung inflammatory resolution versus either AECl (T1a+) cell recovery (H), AECII-to-AECl differentiation (I), or fibrotic lesion regression (J). (C-E): n=4-19 per group; (G): n=3-4 per group. ** $P < 0.01$; *** $P < 0.001$; **** $P < 0.0001$, 1-way ANOVA. Scale bars: 50 μm (B and F-bottom panel); 500 μm (F-top panel).

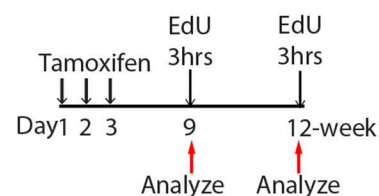
A



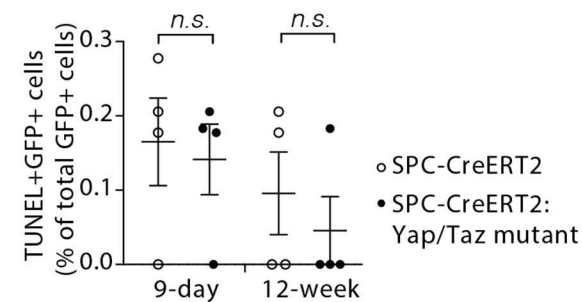
B



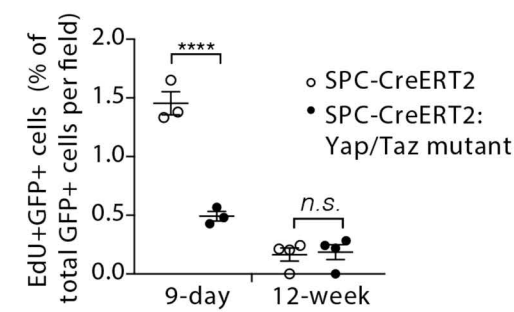
C



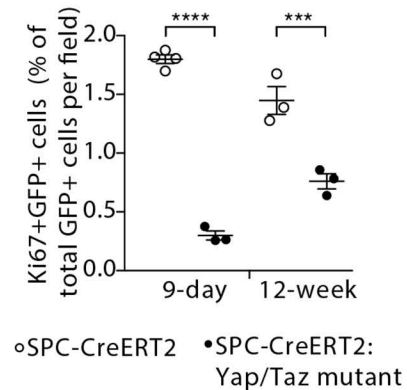
D



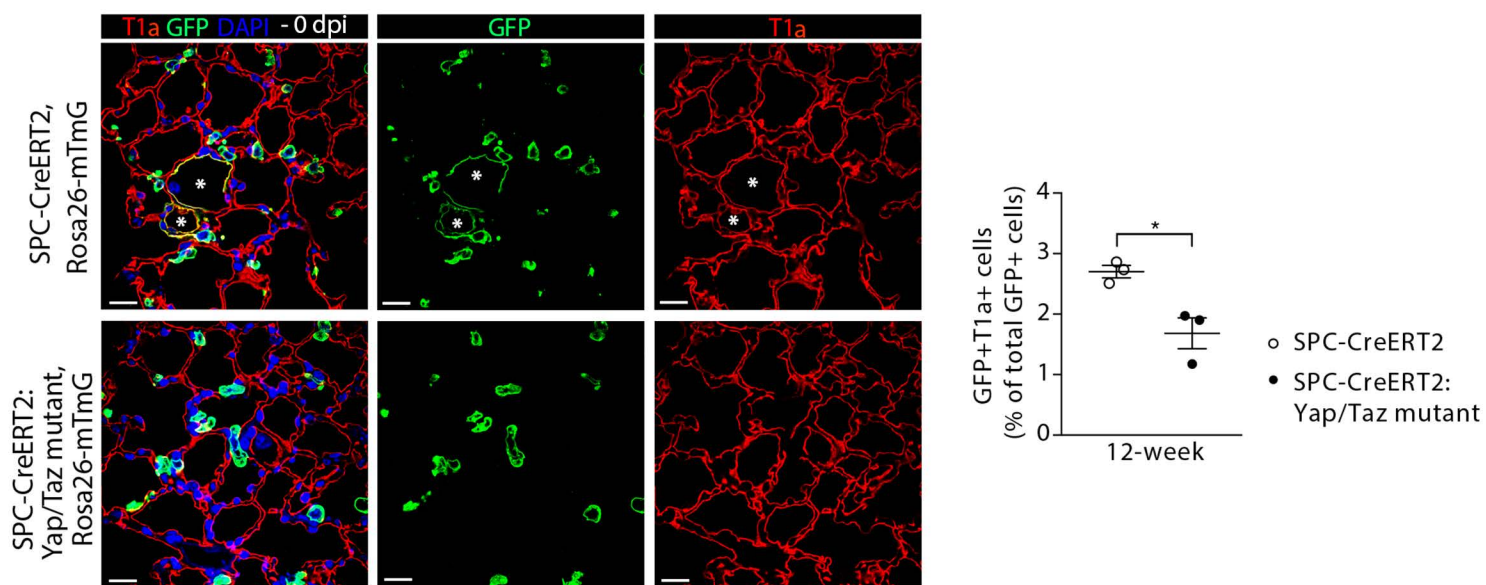
E



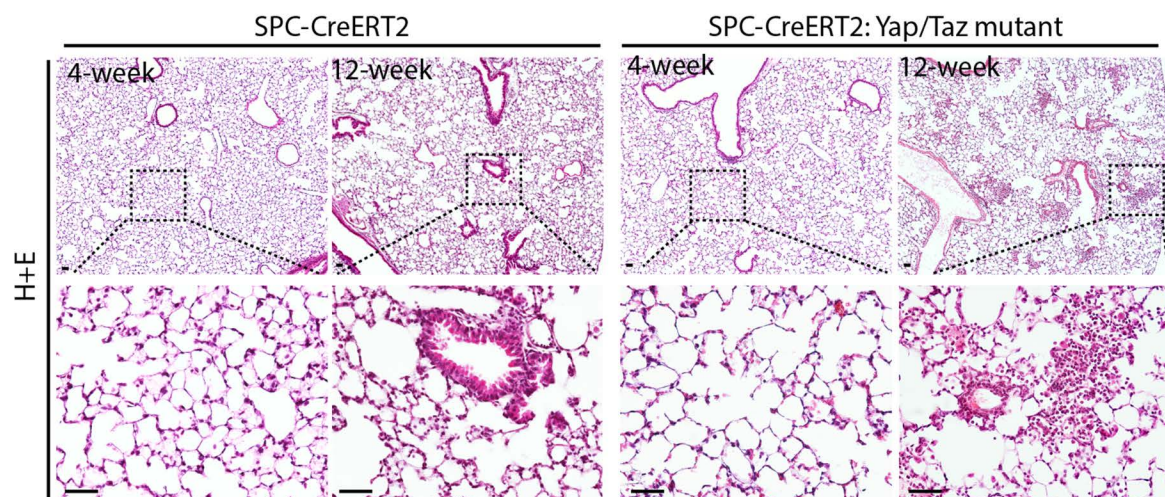
F



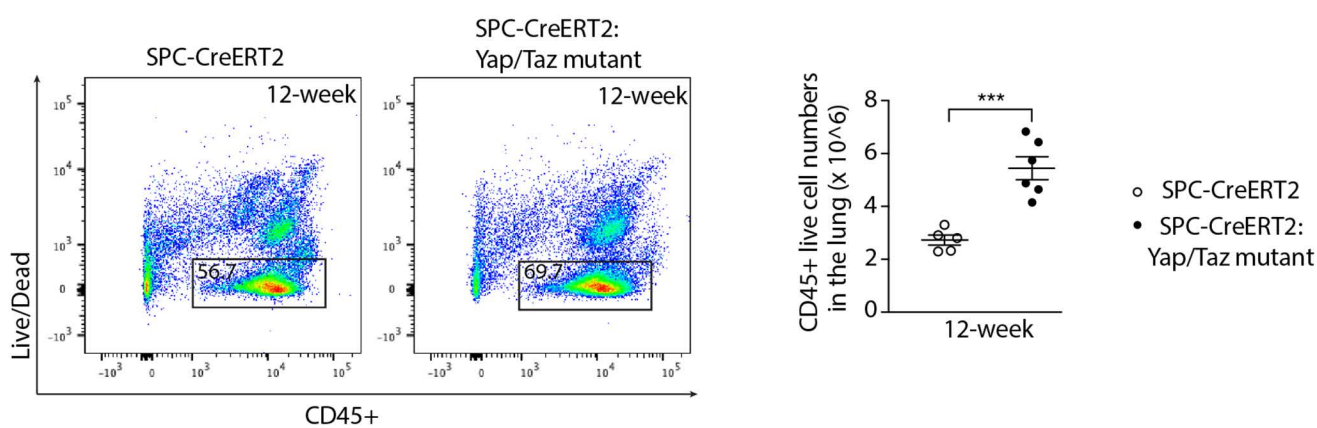
G



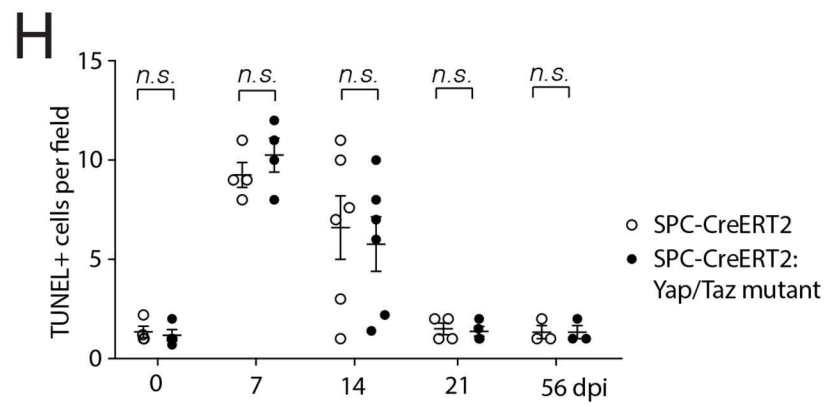
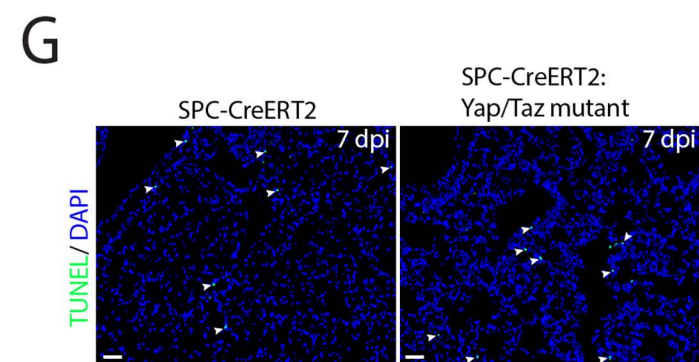
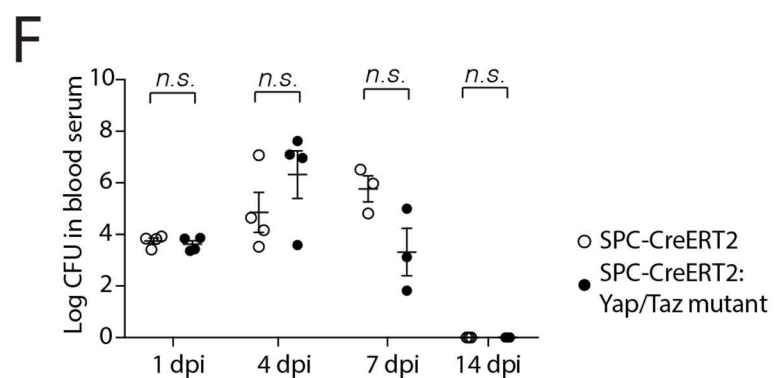
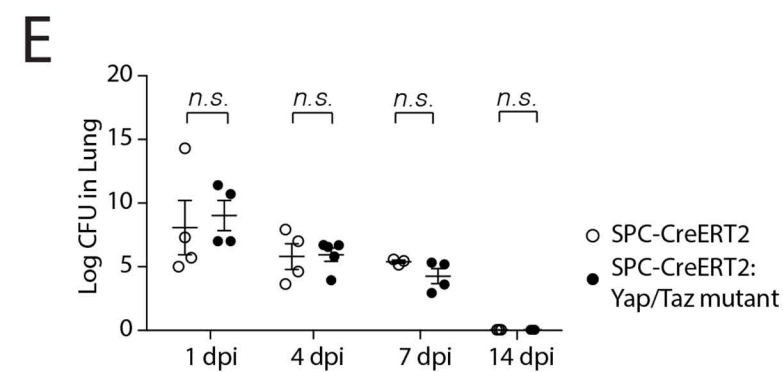
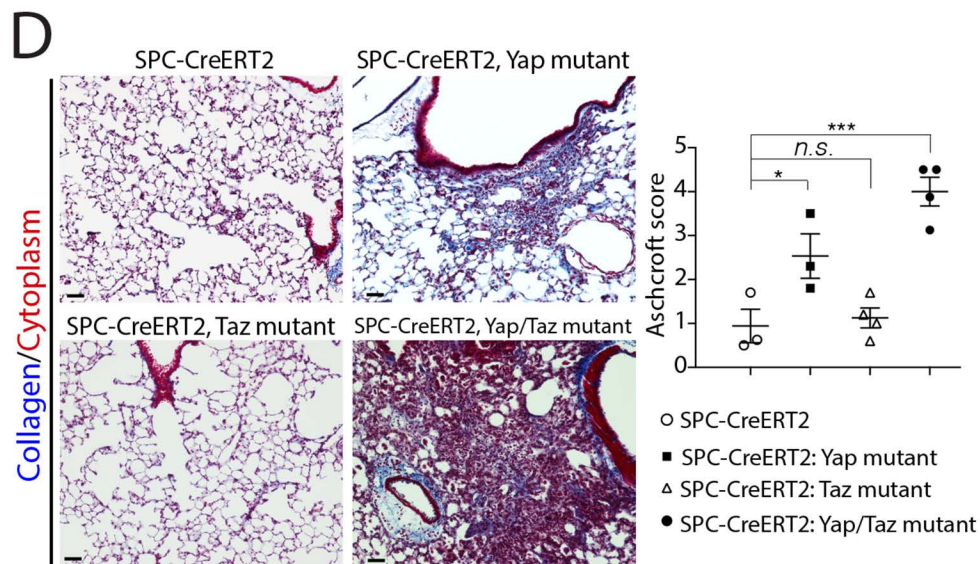
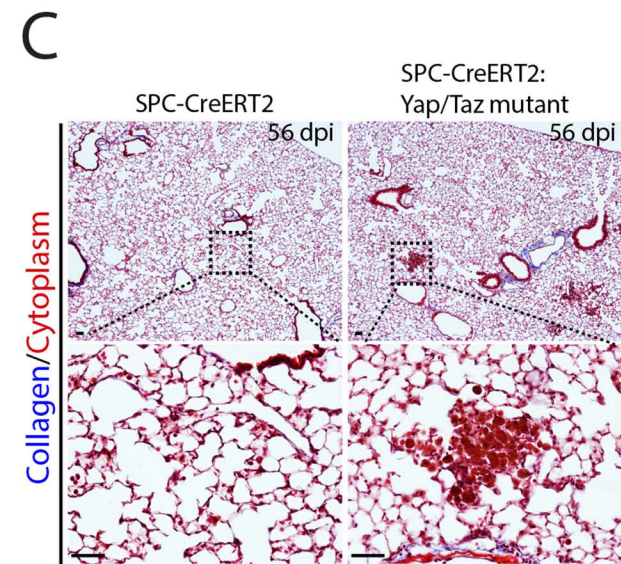
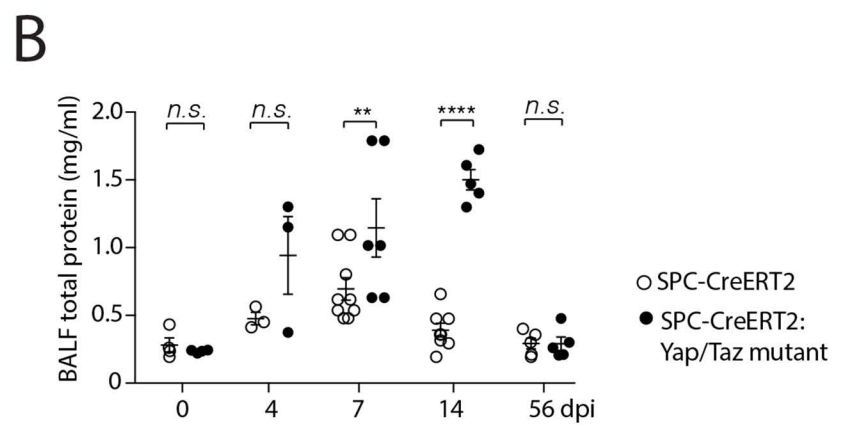
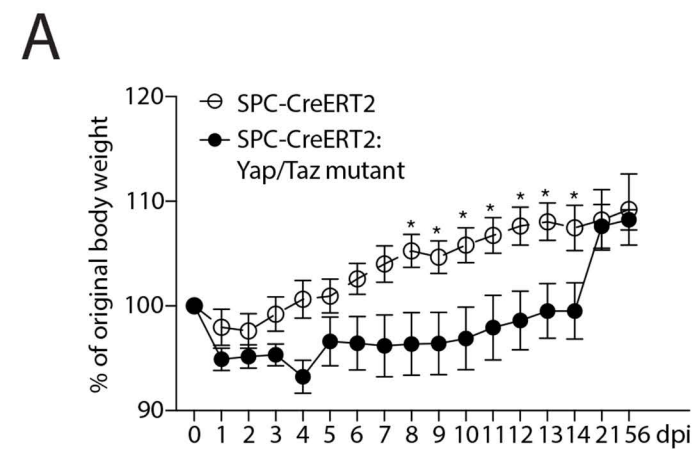
H



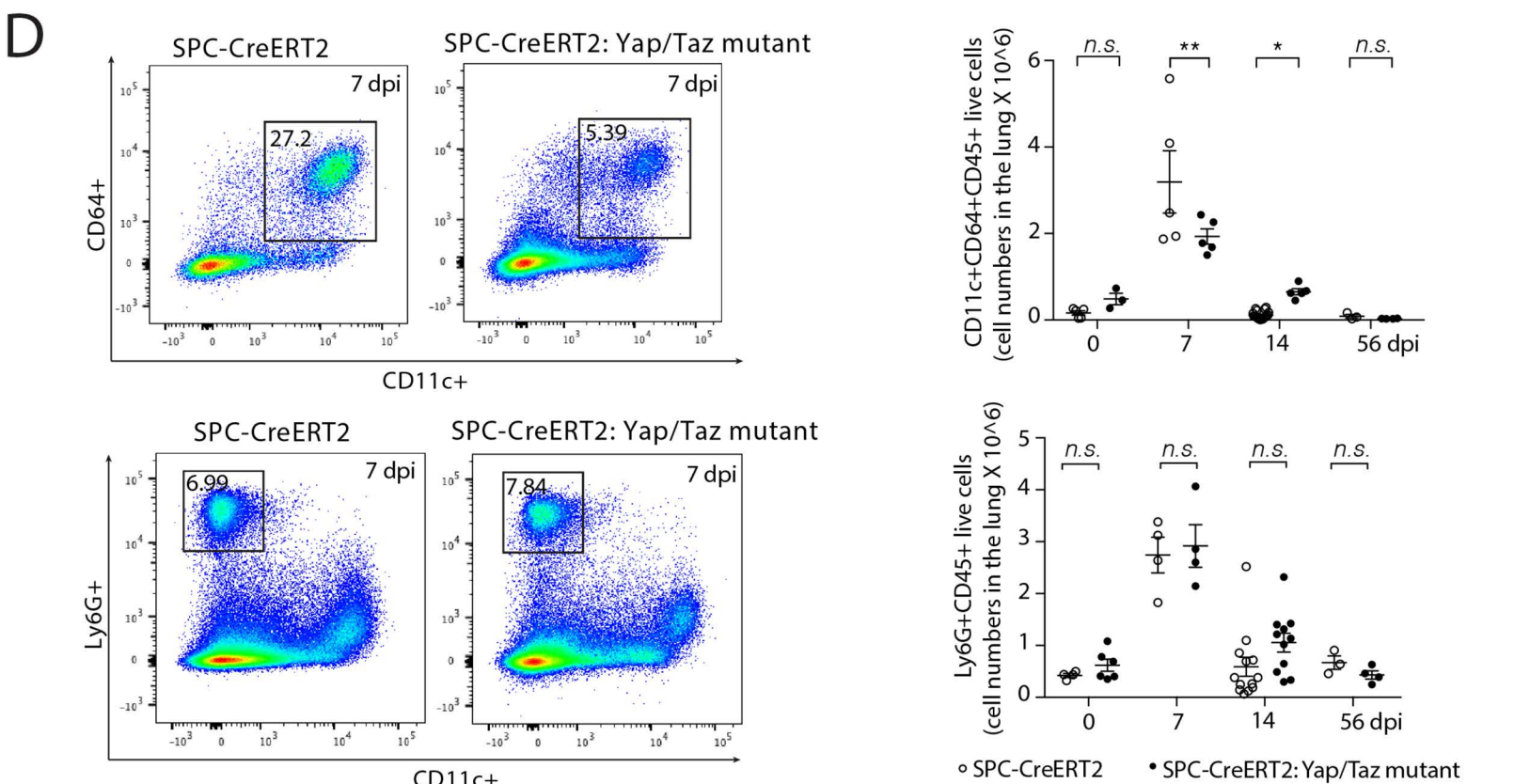
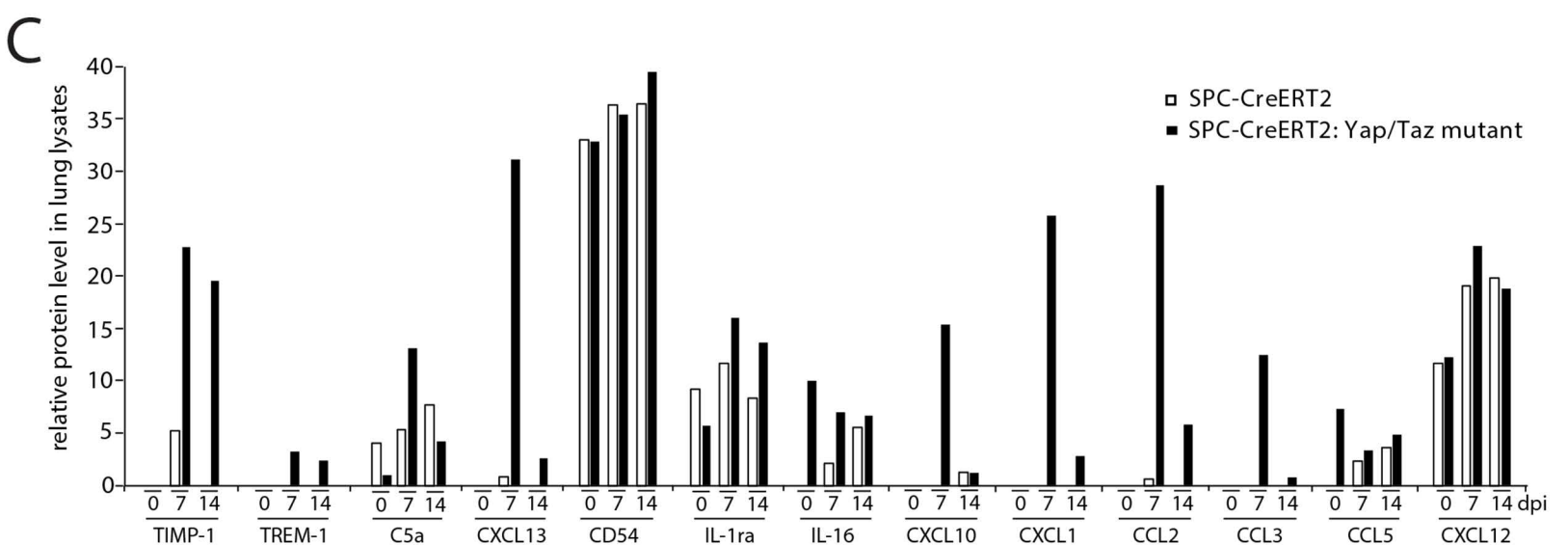
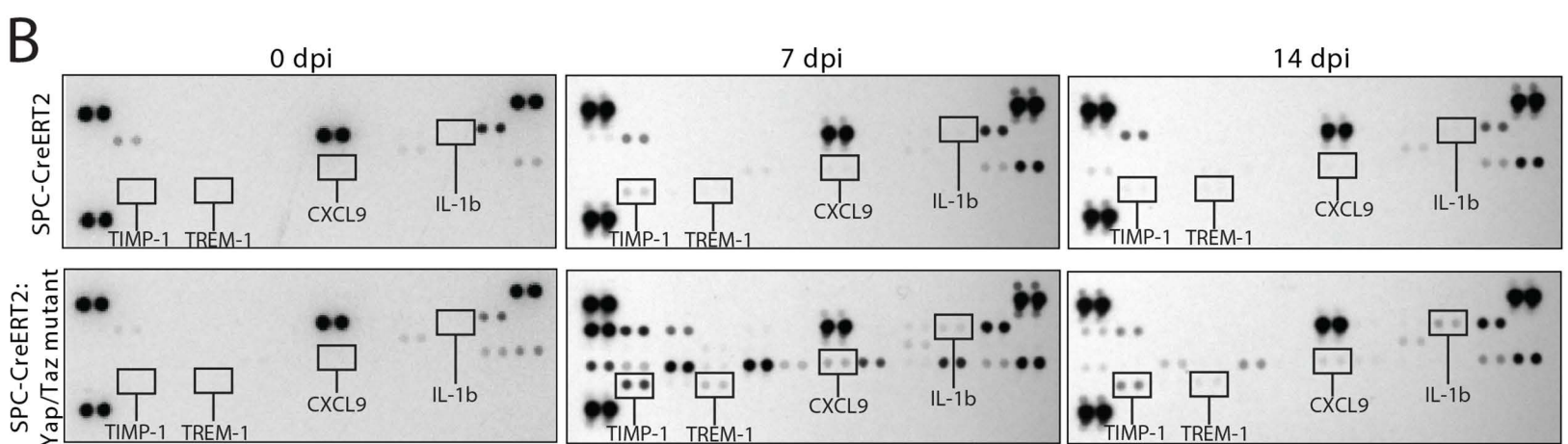
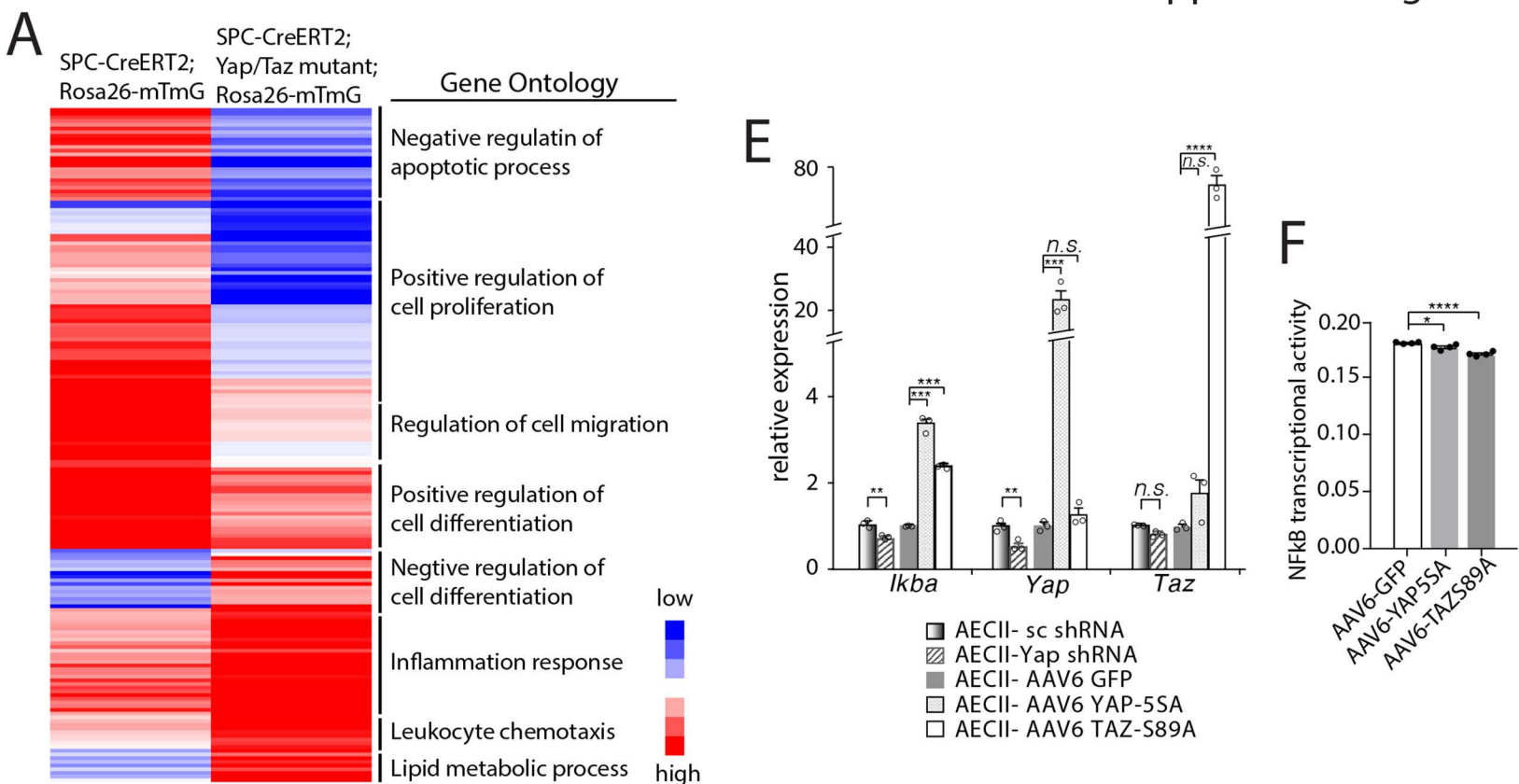
I



Supplemental Figure 3. Effects of Yap/Taz deletion in adult SPC+ AECIIs during homeostasis. (A). Adult SPC-CreERT2, Rosa26-mTmG mice were treated with 3 doses of tamoxifen to label SPC+ AECIIs. Fourteen days after the last tamoxifen treatment, mice were infected with SpT4. Mouse lung epithelial cells were isolated at 0 dpi and 7 dpi and processed for FACS analysis. FACS-sorted GFP+ AECIIs were used for RNA isolation and qRT-PCR analysis. (B) qRT-PCR results showing Yap, Taz, Ctgf, Cyr61 mRNA levels in FACS-sorted GFP+ AECIIs from SPC-CreERT2, Rosa26-mTmG mice or SPC-CreERT2, Yap/Taz mutant, Rosa26-mTmG mice at 0 dpi. (C) Schematic of experimental design for studies performed in (D-H). (D) Quantification of cell apoptosis in the lung by counting TUNEL+ cell numbers on lung sections (≥ 10 randomly selected fields per animal). (E) Quantification of cell proliferation as the percentage of EdU+GFP+ cells of total GFP+ cells on lung sections. (F) Quantification of cell proliferation as the percentage of Ki67+GFP+ cells of total GFP+ cells on lung sections. (G) Confocal images of lung sections at 12 weeks after tamoxifen treatment with immunostaining of anti-GFP (green) and anti-T1a (red), and DNA counterstain (DAPI, blue). Asterisks indicate regions double-positive for GFP and T1a. Percentage of GFP+T1a+ of total GFP+ cells by FACS analysis was graphed (right panel). (H) Images of lung sections with hematoxylin and eosin (H+E) staining at 4 weeks and 12 weeks after tamoxifen treatment. (I) Flow cytometry of dissociated lung cells at 12 weeks after tamoxifen treatment were performed by gating on CD45+ cells. Quantification of CD45+ live cell numbers were graphed (right panel). * $P < 0.05$; ** $P < 0.01$; *** $P < 0.001$; **** $P < 0.0001$, 2-way ANOVA (D-F) and Student's t test (A, B, G, I). (E) and (F) Ten fields per animal and ~ 800 GFP+ cell per animal were analyzed. (A-I): $n=3-6$ per group. Scale bars: 20 μm (G); 50 μm (H).

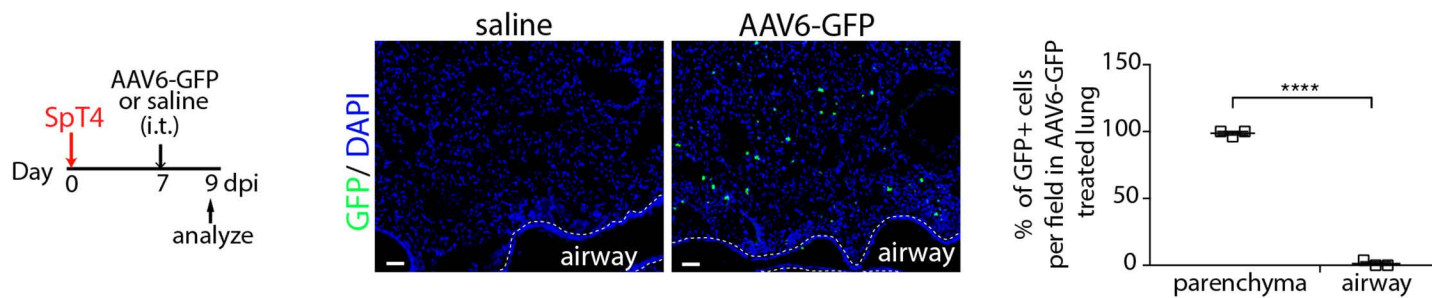


Supplemental Figure 4. Effects of Yap/Taz deletion in adult SPC+ AECIIs during bacterial pneumonia. (A) Mice infected with SpT4 were weighted daily and the percentage change in weight from the baseline was graphed. For 0-14 dpi, n=16 per group; for 21 and 56 dpi, n=4-5 per group. (B) Bronchoalveolar lavage fluids (BALF) were obtained from SpT4-infected mice to measure levels of protein (n=3-9 per group). (C) Mouse lung sections at 56 dpi were stained with Alcian blue and nuclear fast red. (D) Mouse lung sections at 14 dpi were stained with Alcian blue and nuclear fast red. Graph on the right showing lung fibrotic lesions quantified by measuring Aschcroft score (n=3-4 per group). (E) Bacterial loads in lung homogenate measured by CFU plating. (F) Mouse blood serum were obtained and plated for quantitative culture. (G) Mouse lung sections at 7 dpi with TUNEL staining to indicate apoptotic cells. Arrows indicated TUNEL+ cells. (H) Cell apoptosis was quantified by counting TUNEL+ cells on lung sections (≥ 10 randomly selected fields per animal). * $P < 0.05$; ** $P < 0.01$; *** $P < 0.001$; **** $P < 0.0001$, 2-way ANOVA (A, B, E, F, H) and 1-way ANOVA (D). Scale bars: 50 μm (C, D, G).

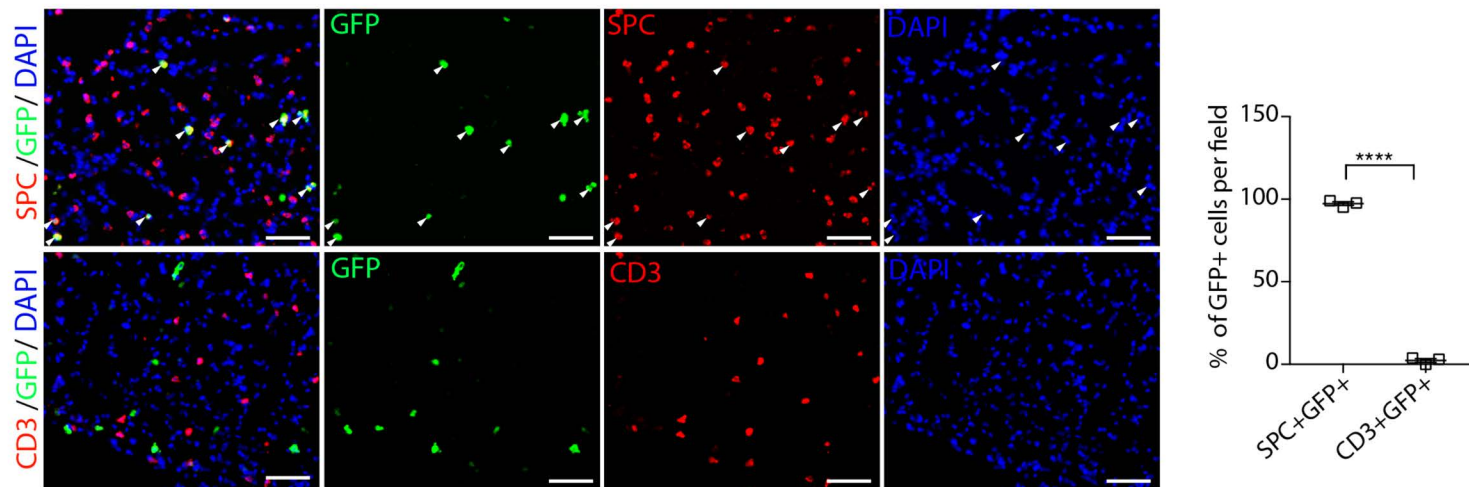


Supplemental Figure 5. Inflammatory responses in Yap/Taz mutant lungs. (A) Heatmap for microarray gene expression data of FACS-sorted GFP⁺ AECIIs from SPC-CreERT2, Rosa26-mTmG and Yap/Taz mutant lungs at 8 dpi. (B) Blot images of cytokine array from whole lung lysates at 0, 7, and 14 dpi. (C) Quantification of cytokine protein levels by densitometry (n=1 per group). (D) Flow cytometry of dissociated lung cells were performed by gating on CD11c⁺CD64⁺CD45⁺ or Ly6G⁺CD45⁺ cells (left panels). Quantification of the number of CD11c⁺CD64⁺CD45⁺ and Ly6G⁺CD45⁺ cells in the lung at 0, 7, 14, and 56 dpi (right panels). (E) AECIIs were purified from adult wild-type mice and cultured with either scrambled shRNA (sc shRNA) lentivirus, Yap shRNA lentivirus, AAV6-GFP, AAV6-YAP-5SA, or AAV6-TAZ-S89A. Forty-eight hours after infection, RNAs were isolated and processed for qRT-PCR analysis (n=3 per group). (F) Adult wild-type mouse AECIIs were purified, cultured and infected with either AAV6-GFP or AAV6-YAP-5SA or AAV6-TAZ-S89A. Forty-eight hours after infection, cells were processed for NF- κ B transcription activity measurement (n=4 per group). * $P < 0.05$; ** $P < 0.01$; *** $P < 0.001$; **** $P < 0.0001$, 2-way ANOVA (D) and 1-way ANOVA (E, F) and Student's t test (E).

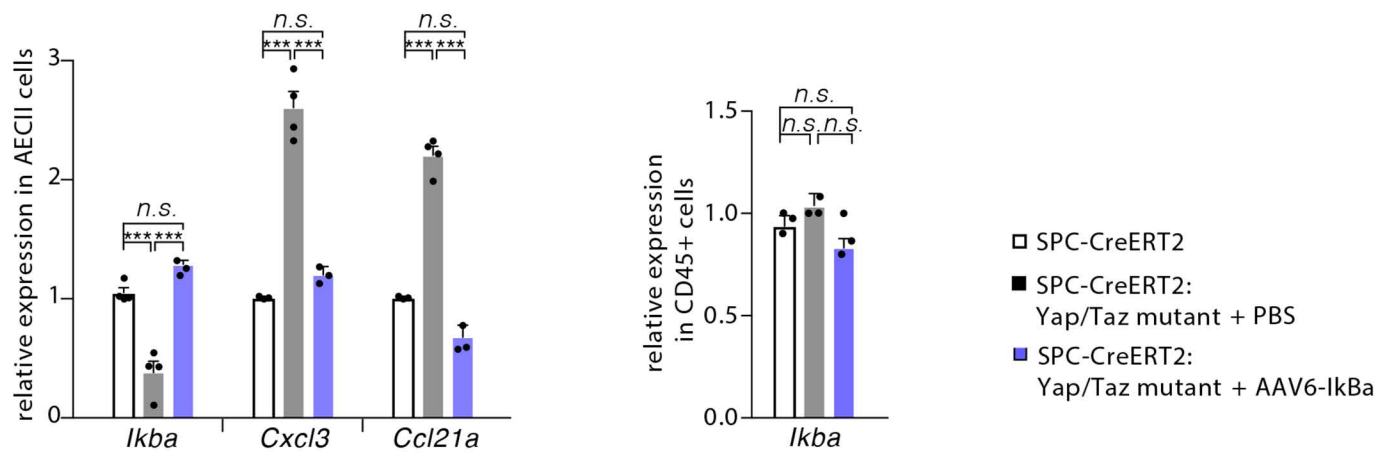
A



B



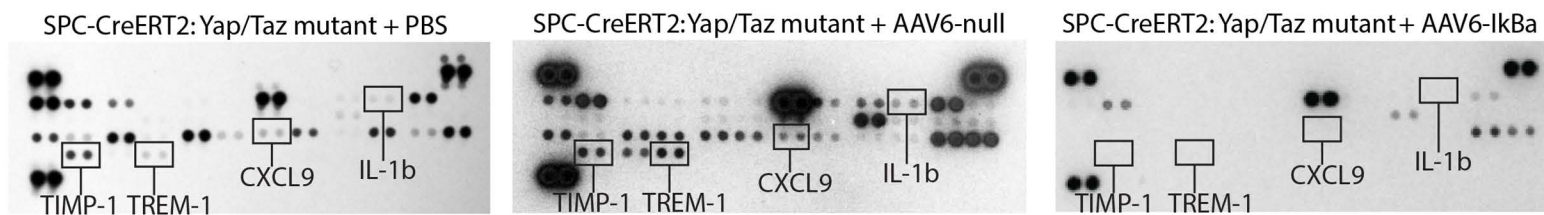
C



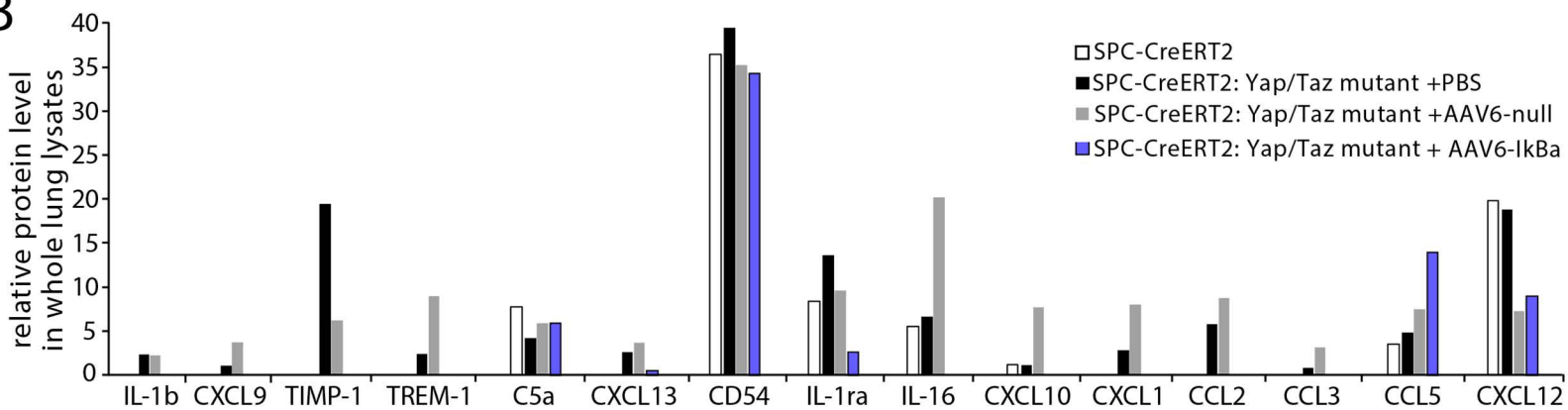
Supplemental Figure 6. AAV6-mediated gene expression in Yap/Taz mutant lungs. (A)

Schematic of experimental design and immunostaining on lung sections with antibody to GFP (green) and DNA counterstain (DAPI, blue). Dashed white lines indicated the airway. Percentage of GFP⁺ cells localized in parenchyma or airway of total GFP⁺ cells were graphed. (B) Images of lung sections with immunostaining of anti-pro-SPC (SPC) (red, top panel), anti-GFP (green), anti-CD3 (red, bottom panel) and DNA counterstain (DAPI, blue). Arrows indicated SPC⁺GFP⁺ cells. Percentage of SPC⁺GFP⁺ or CD3⁺GFP⁺ cells of total GFP⁺ cells were graphed. (C) AECIIs (CD45⁻ EpCAM⁺) and CD45⁺ were purified from adult mouse lungs at 24 hours after AAV6-IkBa or PBS treatment. RNAs were isolated and processed for qRT-PCR analysis (n=3-4 per group). (D) Schematic of experimental design and survival rate of Yap/Taz mutant mice after treatment with either PBS, AAV6-GFP or AAV6-IkBa. ****P* < 0.001; *****P* < 0.0001, Student's t test (A, B) and 1-way ANOVA (C). Scale bars: 50 μm (A and B).

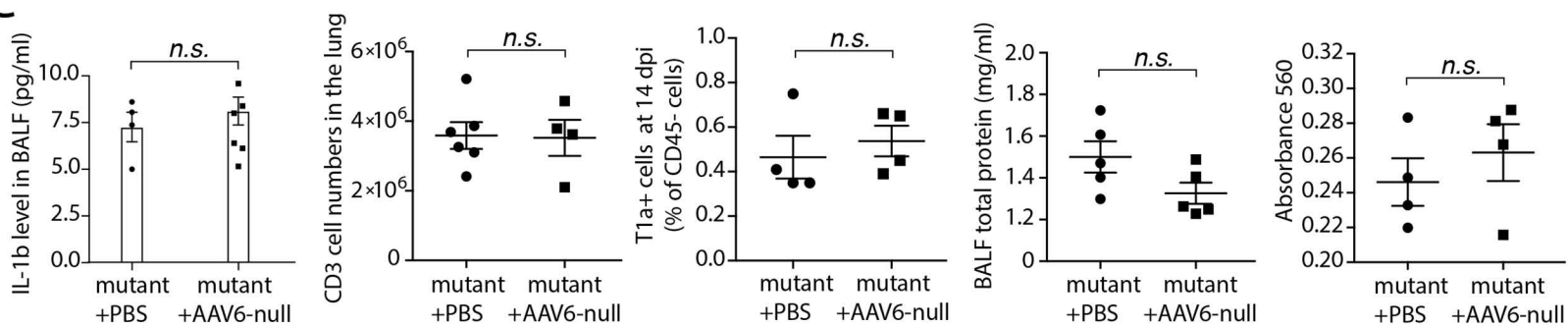
A



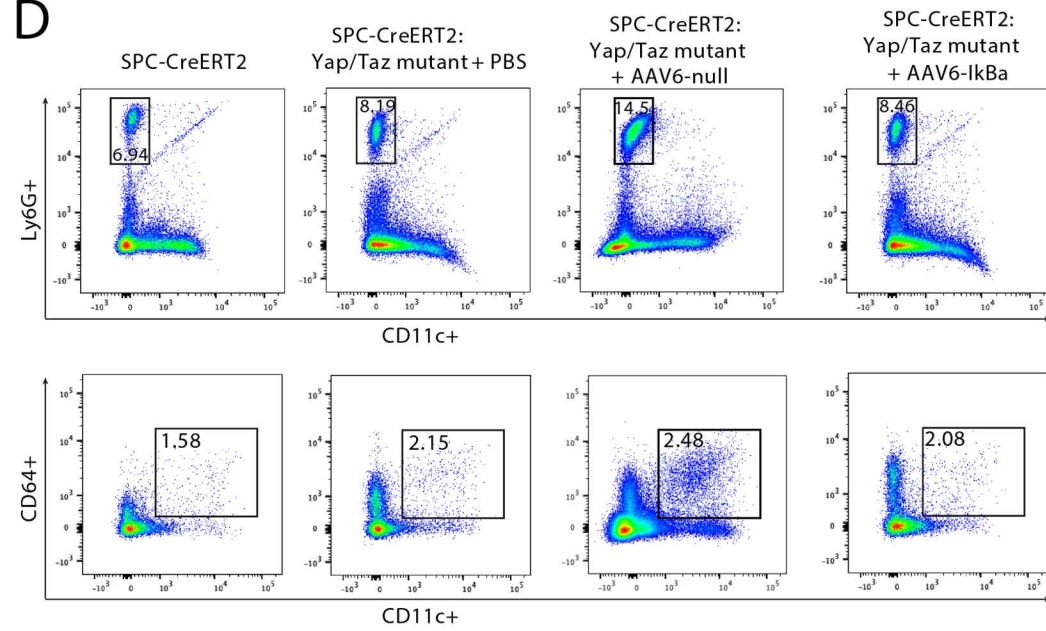
B



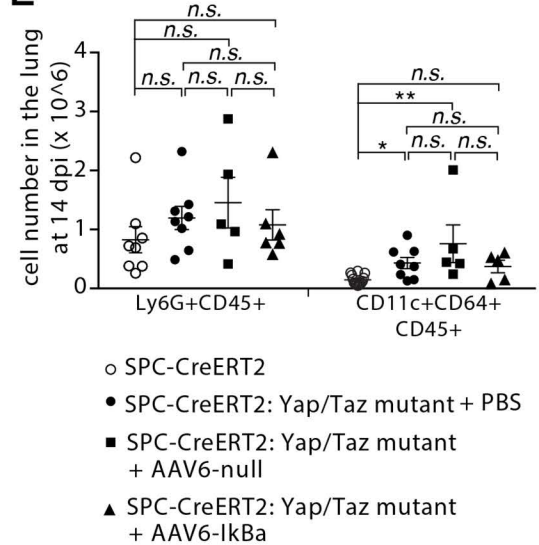
C



D



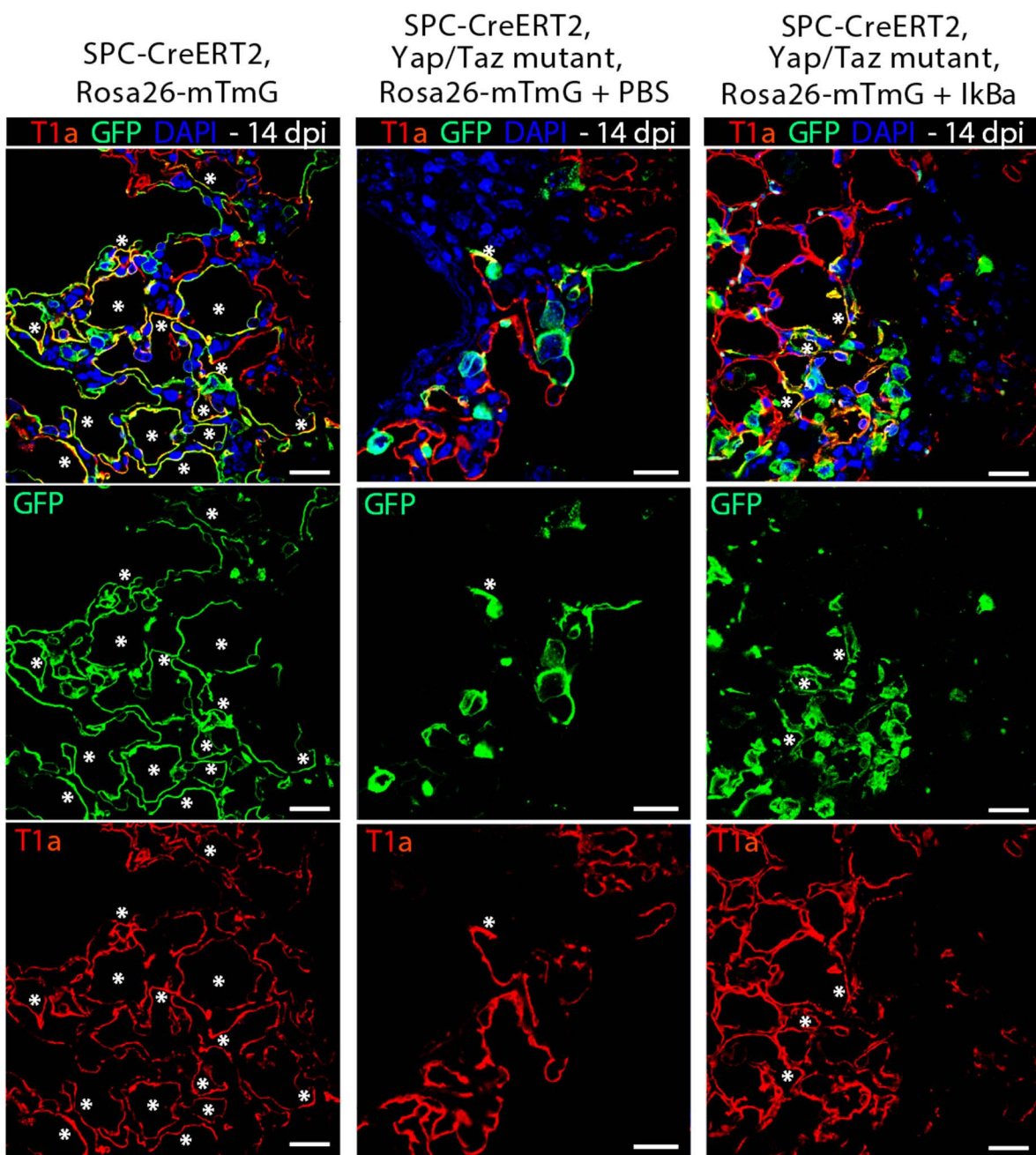
E



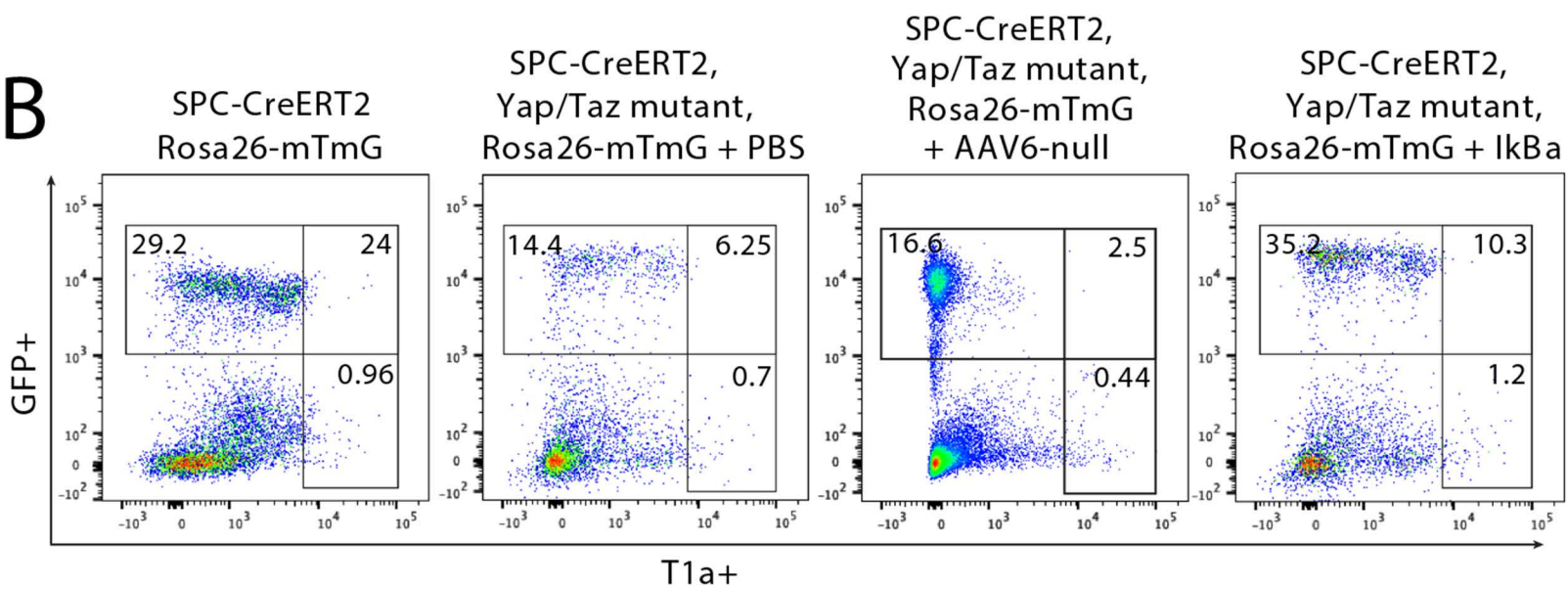
Supplemental Figure 7. Rescue effects of AAV6-IkBa treatment in Yap/Taz mutant lungs.

(A) Blot images of cytokine array from whole lung lysates at 14 dpi. (B) Quantification of cytokine protein levels by densitometry (n=1 per group). (C) PBS-treated Yap/Taz mutant lungs showing similar results as AAV6-null-treated Yap/Taz mutant lungs at 14 dpi, including IL-1b protein level in BALF using ELISA assay, number of CD3⁺ cells and percentage of T1a⁺ cells using flow cytometry, BALF total protein level using BCA assay, and collagen content in lung tissue lysates using hydroxyproline assay (n=4-6 per group). (D) Flow cytometry of dissociated lung cells were performed by gating on Ly6G⁺CD11c⁻CD45⁺ cells (top panels) or CD11c⁺CD64⁺CD45⁺ cells (bottom panels) at 14 dpi. (E) Quantification of number of Ly6G⁺CD45⁺ and CD11c⁺CD64⁺CD45⁺ cells in the lung at 14 dpi (n=5-12 per group). **P* < 0.05; ***P* < 0.01, Student's t test (C) and 1-way ANOVA (E).

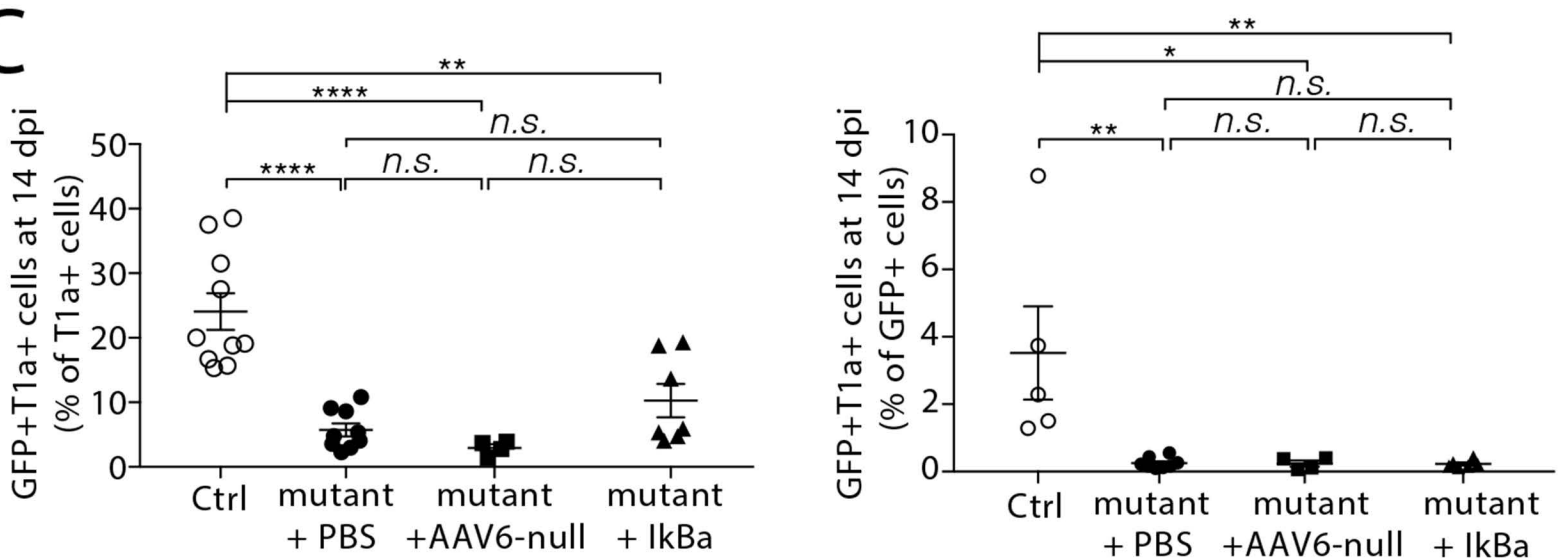
A



B

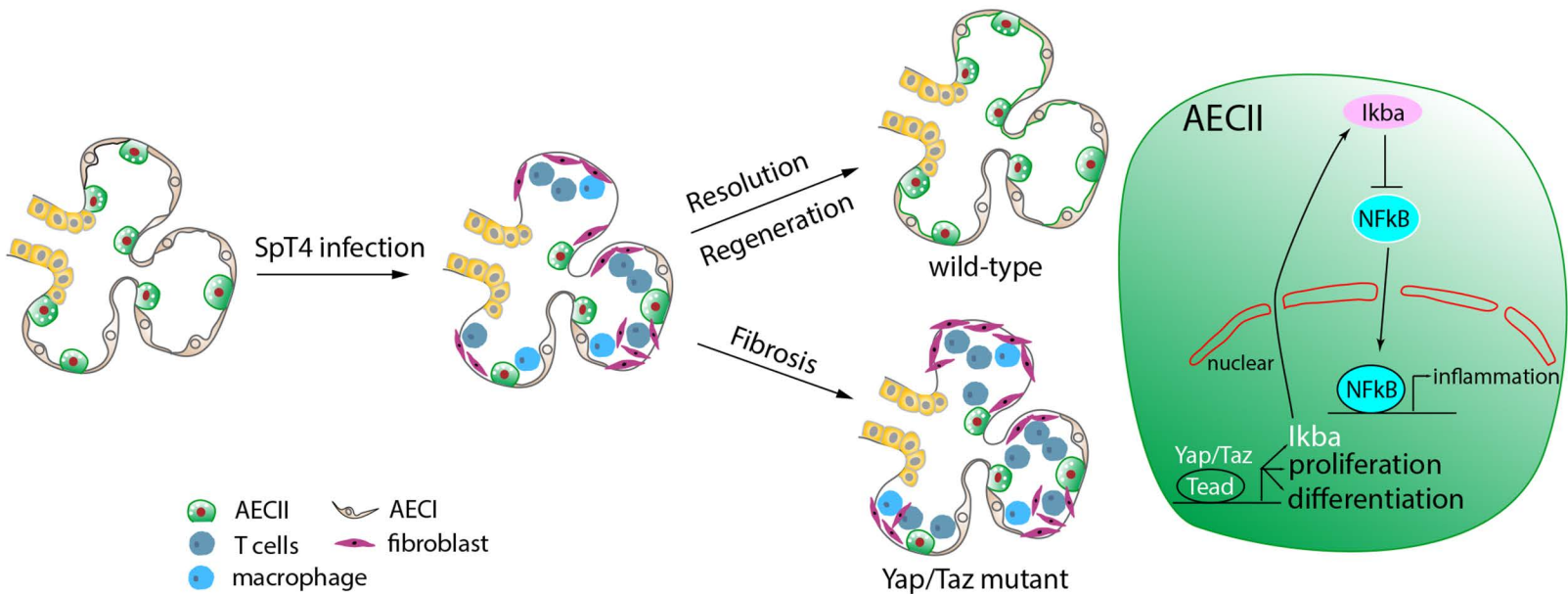


C



- SPC-CreERT2, R26r-mTmG (Ctrl)
- SPC-CreERT2:Yap/Taz mutant, Rosa26-mTmG (mutant)
- SPC-CreERT2:Yap/Taz mutant, Rosa26-mTmG + AAV6-null
- ▲ SPC-CreERT2:Yap/Taz mutant, Rosa26-mTmG + AAV6-IκBa

Supplemental Figure 8. Effects of AAV6-IkBa treatment on AECII differentiation in Yap/Taz mutant lungs. (A) Confocal images on lung sections at 14 dpi with immunostaining of anti-GFP (green), anti-T1a (red) and DNA counterstain (DAPI, blue). Scale bars: 20 μ m. Asterisks indicate regions double-positive for GFP and T1a. (B) Flow cytometry of dissociated lungs were performed by gating on GFP⁺ T1a⁺ cells at 14 dpi. The number in the top left gate represented all GFP⁺ cells of total live CD45⁻ cells. The number in the top right gate represented GFP⁺T1a⁺ cells of total T1a⁺ cells. The number in the bottom right gate represented all T1a⁺ cells of total live CD45⁻ cells. (C) Quantification of percentage of GFP⁺T1a⁺ of total T1a⁺ cells (left panel) or total GFP⁺ cells (right panel) (n=5-10 per group). * $P < 0.05$; ** $P < 0.01$; **** $P < 0.0001$, 1-way ANOVA.



Supplemental Figure 9. Schematic model of Yap/Taz-IkBa axis during alveolar regeneration and resolution of lung inflammation.